Adaptive Neural Network Control of a Robotic Manipulator with Unknown Backlash-like Hysteresis

Wei He[1,*], David Ofosu Amoateng[2], Chenguang Yang[3], Dawei Gong[4]

[1]School of Automation and Electrical Engineering and the Key Laboratory of Advanced Control of Iron and Steel Process, , University of Science and Technology Beijing, Beijing 100083, China.
[2]Department of Electrical Engineering and Computer Science, Masdar Institute of Science and Technology, Abu Dhabi, UAE
[3]Zienkiewicz Centre for Computational Engineering, Swansea University, Swansea, SA1 8EN, United Kingdom
[4]School of Mechatronics Engineering, University of Electronic Science and Technology of China, Chengdu 611731, China
[*]weihe@ieee.org. This work was supported by the National Natural Science Foundation of China under Grant 61522302, the National Basic Research Program of China (973 Program) under Grant 2014CB744206, the National High Technology Research and Development Program of China (863 Program) under Grant 2015AA042304, and the Fundamental Research Funds for the China Central Universities of USTB under Grant FRF-TP-15-005C1.

Abstract: This paper proposes an adaptive neural network controller for a 3-DOF robotic manipulator that is subject to backlash-like hysteresis and friction. Two neural networks to approximate the dynamics and the hysteresis nonlinearity. A neural network, which utilizes a radial basis function approximates the robot's dynamics. Another neural network, which employs a hyperbolic tangent activation function, is used to approximate the unknown backlash-like hysteresis. We also consider two cases: full state and output feedback control. For output feedback, where system states are unknown, a high gain observer is employed to estimate the states. The proposed controllers ensure the boundedness of the control signals. Simulations are also performed to show the effectiveness of the controllers.

Keywords: Neural Networks, Adaptive Control, Robotic Manipulator, Hysteresis, Backlash.

1. Introduction

Backlash hysteresis is quite present in many systems such as gear systems and actuators. It occurs when the direction of motion of an actuated joint is reversed [1]. Although backlash hysteresis is required in geared transmission for proper tooth action, too much backlash may degrade system performance and produce oscillations that can cause instability. Designing control systems without compensating backlash hysteresis can damage the system. Numerous models and methods

have been proposed and more are being studied to help compensate backlash hysteresis and other nonlinearities in nonlinear systems [2–4]. In [4], the authors propose an adaptive output feedback controller for a nonlinear hysteresis system. They prove that the control scheme is effective in removing the effects of hysteresis. Some of these techniques require the use of an inverse function. The Preisach model and the Prandtl-Ishlinskii model are two well known models for simulating backlash hysteresis [5–7]. In [5], an approach to modelling robotic joints with hysteresis and backlash is presented. A Preisach operator is used to model the hysteresis in the joints. A modified Prandtl-Ishlinskii model for compensating asymmetric hysteresis is proposed in [6]. The model is compared with a classical Prandtl-Ishlinskii model and showed a 66% decrease in error. In [8], a Preisach model is used to simulate the hysteric behaviour of piezoceramic actuators. The inverse Preisach model is used together with a controller to control the system. Simulation shows that the error reduces by 50% to 70% compared to systems without hysteresis compensation. In [9], Yi et al considered hysteresis as disturbance. Using a disturbance observer, hysteresis is estimated and compensated for. Their method does not require an inverse model and is very simple.

In [10], a nonlinear controller which is very robust is proposed to overcome deadzone nonlinearities which are present in many physical systems. An ideal reference output is generated using an ideal model of the system. Through simulations, the authors show that the controller achieves satisfactory system performance. In [11], a controller is proposed to overcome input saturation. The controller is formulated using backstepping technique and Lasalle's invariance principle. Computer simulations and experiments confirm the validity of the proposed laws. In [12], hysteresis is compensated in piezoelectric actuators using neural networks. The control problem is designed as an optimization problem and solved using the Levenberg-Marquardt algorithm. Experiments show good tracking and control performance for the proposed scheme. In [13], hysteresis backlash is described by a dynamic differential equation. The controller is developed using the solution properties of the hysteresis dynamic differential equation. The control law ensures global stability and strict tracking precision. This method, however, requires the system to be within known bounds or intervals. Two control schemes are proposed in [14]. The backlash hysteresis takes into account external disturbances. The first scheme uses a sliding mode controller which employs a

sign function. The sign function however causes chattering. The second adaptive control scheme employs a continuous function. Unlike other control techniques, the two schemes in [14] do not require parameters of the model and the disturbance-like term to be within certain bounds.

In some situations, the system states cannot be measured. There are some control schemes and methods that approximate system states [15, 16]. Zhou et al. [17] also propose an output feedback control scheme by incorporating in the controller design, an inverse model which eliminates hysteresis. In [18], neural networks are used to approximate the dynamics of a robot subject to input deadzone and output constraint. The output feedback controller estimates system states without violating the set constraints. An adaptive fuzzy output feedback controller is proposed in [19]. The nonlinear system considered has unmeasured states and unknown dynamics. The fuzzy logic controller employed completely identifies the unknown nonlinear function. Simulations are also provided to show the effectiveness of the proposed control method. In [20], a simple procedure using a nonlinear compensator is proposed. The compensator eliminates limit cycles which arise due to hysteresis or backlash in contactors. The technique effectively removes the backlash and does not alter the deadzone.

Most of these hysteresis models and most nonlinear models are very complicated and difficult to construct. Learning algorithms are very useful when constructing controllers for systems with unknown models. [21–26]. An approximation based algorithm is given in [27]. The complex dynamics and nonlinear terms of the robot is compensated by a RBFNN. In [28], a neural network controller for proper coordination of a humanoid robot which considers hysteresis is presented. The adaptive neural network approach guarantees very good tracking performance. Selmic et al. [29], also use an inversion approach to approximate the hysteresis function. Geng et al. [30] use a neural network to compensate hysteresis and improve the precision of a nanometer positioning system. An inverse model is coupled with the hysteresis model, as a filter to remove the effects of hysteresis. The nonlinear characteristic is effectively reduced, which results in a more linear output. In [31], a neural network compensates hysteresis and in position controlled mechanisms. The neural network switches to a smoother control when torque transmitted to the shaft is reversed. In [32], a novel Takagi-Sugeno (T-S) fuzzy-system- based model is proposed for hys-

teresis in piezoelectric actuators using an inverse hysteresis model to develop the fuzzy controller. The controller also utilizes least sqaure algorithm for optimization. Zhi et al [33], investigate the control of time delayed continuous nonlinear systems subject to hysteresis. The controller adopts an optimized adaptation method to reduce computational burden. Numerical simulations provided show the effectiveness of the proposed scheme.

2. Problem Formulation and Preliminaries

The dynamics of an n-link robotic manipulator can be expressed as [34]:

$$M(q)\ddot{q} + C(q,\dot{q})\dot{q} + F(\dot{q}) + G(q) = \phi(\tau) \tag{1}$$

where $q \in \mathbb{R}^n$ is a vector of joint variables, $\phi(\tau) \in \mathbb{R}^n$ represents the backlash hysteresis input. $M(q) \in \mathbb{R}^{n\times n}$ is the inertia matrix, $C(q,\dot{q}) \in \mathbb{R}^{n\times n}$ represents the Coriolis and centrifugal matrix, $F(\dot{q}) \in \mathbb{R}^n$ is the friction term and $G(q) \in \mathbb{R}^n$ is the gravitational force.

Property 1. [35] The matrix $V(q,\dot{q})$ is skew-symmetric, where $V(q,\dot{q}) = \dot{M} - 2C(q,\dot{q})$ is. Therefore $x^T V x = 0 \, \forall x \in \mathbb{R}^n$.

Property 2. [36] The friction term can be approximated as:

$$F(\dot{q}) = F_v\dot{q} + F_d(\dot{q}) \tag{2}$$

where $F_v \in \mathbb{R}^{n\times n}$ and $F_d(\dot{q}) \in \mathbb{R}^n$ denotes the viscous friction coefficients and coulomb friction coefficients.

Property 3. The backlash input nonlinearity is defined as [37]:

$$\frac{d\phi_i(\tau_i)}{dt} = h_{ri}\left|\frac{d\tau_i}{dt}\right|[h_{ai}\tau_i - \phi_i(\tau_i)] + h_{bi}\frac{d\tau_i}{dt} \tag{3}$$

h_{ri}, h_{ai} and h_{bi} are constants and $h_{ai} > 0$ is the slope satisfying $h_{ai} > h_{bi}$. According to [13], (3)

can be solved as

$$\begin{aligned} \phi_i(\tau(t)) &= h_{ai}\tau_i(t) + d_i(\tau_i), \qquad i = 1, 2...n \quad (4) \\ d_i(\tau_i) &= [\phi_i(\tau_i)(0) - h_{ai}\tau_i(0)]e^{-h_{ri}(\tau_i - \tau_i(0))sgn(\dot{\tau}_i)} \\ &\quad + e^{-h_{ri}\tau_i sgn(\dot{\tau}_i)} \int_{\tau_i(0)}^{\tau_i} [h_{bi} - h_{ai}]e^{-h_{ri}\zeta_j sgn(\dot{\tau}_i)} d\zeta_j \quad (5) \end{aligned}$$

This shows that (3) can be used to represent backlash-like hysteresis as illustrated in Fig. 1, where $h_{ri} = 1$, $h_{ai} = 3.15$, $h_{bi} = 0.35$, $\tau_i(t) = x\sin(2.3t), \quad x = 2.5, 3.5, 4.5$. As illustrated in [13], $d_i(\tau_i)$ is bounded, i.e $|d_i(\tau_i)| \leq d_i^*$. The backlash hysteresis input nonlinearity $\phi(\tau)$, is expressed

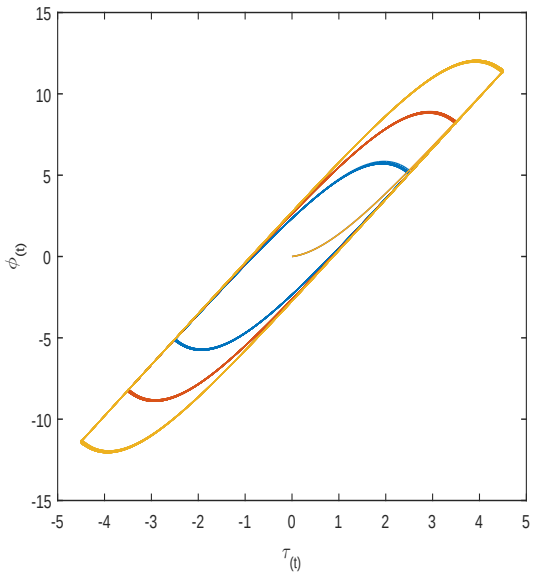

Fig. 1. *Hysteresis curves*

as

$$\phi(\tau) = H_a\tau + D(\tau) \quad (6)$$

where H_a = diag$\{h_{ai}, h_{a2}, ...h_{an}\} > 0$ and $D(\tau) = [d_1(\tau_i), d_2(\tau_2), ...d_n(\tau_n)]^T$ with $\|D(\tau)\| \leq D^*$ with $D^* = \sqrt{d_1^{*2} + d_2^{*2} + ... + d_n^{*2}}$.

Assumption 1. [38] The slope of the backlash like hysteresis H_a and the inertia matrix are

unknown, but there exists positive constants $\bar{h}_a^*$, h_a^* and m^* such that $\bar{h}_a^* \leq \| \ H_a \ \| \leq \ h_a^*$ and $||M|| \leq m*$.

3. Control Design

3.1. Full State Feedback Control

The case where all state information is assumed to be available is first presented. From (1), if we let $x_1 = [q_1, q_2..., q_n]^T$ and $x_2 = [\dot{q}_1, \dot{q}_2..., \dot{q}_n]$, robot manipulator dynamics is rewritten as:

$$\begin{aligned} \dot{x}_1 &= x_2 \\ \dot{x}_2 &= M^{-1}[H_a\tau + D(\tau) - C(x_1, x_2)x_2 - F(x_2) - G(x_1)] \end{aligned} \tag{7}$$

Let the error variable e_1 be defined as

$$e_1 = x_1 - x_d \tag{8}$$

where x_d is the desired trajectory. Its time derivative is defined as

$$\dot{e}_1 = \dot{x}_1 - \dot{x}_d \tag{9}$$

We define a second error variable

$$e_2 = x_2 - \alpha \tag{10}$$

Its time derivative is

$$\dot{e}_2 = \dot{x}_2 - \dot{\alpha} \tag{11}$$

Selecting a Lyapunov function V_1 as

$$V_1 = \frac{1}{2} e_1^T e_1 \tag{12}$$

Differentiating yields

$$\dot{V}_1 = e_1^T \dot{e}_1 = e_1^T (e_2 + \alpha - \dot{x}_d) \tag{13}$$

We can choose the virtual control as

$$\alpha = \dot{x}_d - K_1 e_1 \tag{14}$$

Substituting (14) into (13) yields

$$\dot{V}_1 = -e_1^T K_1 e_1 + e_1^T e_2 \tag{15}$$

Choosing another function

$$V_2 = V_1 + \frac{1}{2} e_2^T H_a^{-1} M e_2 \tag{16}$$

Differentiating V_2 yields

$$\dot{V}_2 = \dot{V}_1 + e_2^T H_a^{-1} M \dot{e}_2 + \frac{1}{2} e_2^T H_a^{-1} \dot{M} e_2 \tag{17}$$

Substituting (8) and (11) into (17) and applying property 1 yields

$$\begin{aligned} \dot{V}_2 &= \dot{V}_1 + e_2^T [\tau + H_a^{-1} D(\tau) - H_a^{-1} (C(e_2 + \alpha) \\ &\quad + G(x_1) + F(x_2) + M\dot{\alpha})] + \frac{1}{2} e_2^T H_a^{-1} \dot{M} e_2 \\ &= -e_1^T K_1 e_1 + e_1^T e_2 + e_2^T [\tau + Q(X) + H_a^{-1} D(\tau)] \end{aligned}$$

where $Q(X) = -H_a^{-1}(C\alpha + G(x_1) + F(x_2) + M\dot{\alpha})$ and $X = [x_1^T, x_2^T, \alpha^T, \dot{\alpha}^T]^T$. However most of these terms such as C, M and F are quite difficult to determine. A neural network which employs a radial basis function will approximate these unknown terms.

$$Q(X) = W^{*T} S(X) + \epsilon_z \tag{18}$$

where $W^{*T} \in \mathbb{R}^{l \times n}$ is an ideal weight matrix, l is the number of neural nodes, ϵ_z is the error of approximation with $\|\epsilon_z\| \leq \epsilon_z^*$ and $\epsilon_z^* > 0$. W^{*T} is not known, therefore, $\hat{W}^T$ will be used to design the controller. We propose the controller as

$$\tau = -e_1 - K_2 e_2 - \hat{W}^T S(X) - \hat{\beta} \tanh(\frac{e_2}{b}) \tag{19}$$

The network updating law is designed as

$$\dot{\hat{W}} = \Gamma_w (S(X) e_2^T - \sigma_w \hat{W}) \tag{20}$$

$$\dot{\hat{\beta}} = \Gamma_\beta (\tanh(\frac{e_2}{b}) e_2^T - \sigma_\beta \hat{\beta}) \tag{21}$$

where $K_1 \in \mathbb{R}^{n \times n}$ and $K_2 \in \mathbb{R}^{n \times n}$ are diagonal and positive, $\hat{\beta} \in \mathbb{R}^{n \times n}$ is the estimate of $\beta^* = \lambda_\beta I$ with $\lambda_\beta = \epsilon_z^* + \|H_a^{-1}\| D^*$. $\Gamma_w = \Gamma_w^T \in \mathbb{R}^{l \times l}$, $\Gamma_\beta = \Gamma_\beta^T \in \mathbb{R}^{n \times n}$, σ_w, σ_β and b are positive constants. $S(X)$, the radial basis function is defined as

$$S_j(X) = \exp\left[\frac{-(X - \mu_j)^T (X - \mu_j)}{\eta_j^2}\right], \quad j = 1, 2, ..., l \tag{22}$$

where μ is the mean and η is the variance of the radial basis function.

For this updating law, the σ term makes the system more robust [18, 39]. $\tilde{W}$ and $\tilde{\beta}$ are denoted as $\hat{W} - W^*$ and as $\hat{\beta} - \beta^*$ respectively. Considering the effects of $\tilde{\beta}$ and $\tilde{W}$ on stability, the function below is selected.

$$V_3 = V_2 + tr\{\frac{1}{2} \tilde{W}^T \Gamma_w^{-1} \tilde{W}\} + tr\{\frac{1}{2} \tilde{\beta}^T \Gamma_\beta^{-1} \tilde{\beta}\} \tag{23}$$

Differentiating V_3 yields

$$\dot{V}_3 = \dot{V}_2 + tr\{\tilde{W}^T\Gamma_w^{-1}\dot{\hat{W}}\} + tr\{\tilde{\beta}\Gamma_\beta^{-1}\dot{\hat{\beta}}\} \tag{24}$$

Substituting (18) , (19), (20) and (21) into (24) yields

$$\begin{aligned}\dot{V}_3 &= -e_1^T K_1 e_1 - e_2^T K_2 e_2 - e_2^T \beta^* \tanh(\frac{e_2}{b}) \\ &\quad + e_2^T[\epsilon_z + H_a^{-1}D(\tau)] - \sigma_w tr\{\tilde{W}^T\hat{W}\} - \sigma_\beta tr\{\tilde{\beta}^T\hat{\beta}\}\end{aligned}$$

Denote $\beta = \epsilon_z + H_a^{-1}D(\tau) \triangleq [\beta_1, \beta_2, ...\beta_n]^T$. The following property holds: $|\beta_i| \leq \|\beta\| \leq \|\epsilon_z\| + \|H_a^{-1}\|\|D(\tau)\| \leq \lambda_\beta, \forall_i = 1, 2, ...n$. This implies that

$$e_2^T[\epsilon_z + H_a^{-1}D(\tau)] = \sum_{i=1}^{n} e_{2i}\beta_i \leq \lambda_\beta \sum_{i=1}^{n} |e_{2i}| \tag{25}$$

Considering (25) and using the facts that

$$\begin{aligned}-\sigma_w tr\{\tilde{W}^T\hat{W}\} &\leq -\frac{\sigma_w}{2}\|\tilde{W}\|_F^2 + \frac{\sigma_w}{2}\|W^*\|_F^2 \\ -\sigma_\beta tr\{\tilde{\beta}^T\hat{\beta}\} &\leq -\frac{\sigma_\beta}{2}\|\tilde{\beta}\|_F^2 + \frac{\sigma_\beta}{2}\|\beta^*\|_F^2\end{aligned}$$

we have

$$\begin{aligned}\dot{V}_3 &\leq -e_1^T K_1 e_1 - e_2^T K_2 e_2 + \lambda_\beta \sum_{i=1}^{n} |e_{2i}| - \lambda_\beta e_2^T \tanh(\frac{e_2}{b}) \\ &\quad -\frac{\sigma_w}{2}\|\tilde{W}\|_F^2 + \frac{\sigma_w}{2}\|W^*\|_F^2 - \frac{\sigma_\beta}{2}\|\tilde{\beta}\|_F^2 + \frac{\sigma_\beta}{2}\|\beta^*\|_F^2\end{aligned}$$

Using the equality and inequality below

$$-\lambda_\beta e_2^T \tanh(\frac{e_2}{b}) = -\lambda_\beta \sum_{i=1}^{n}[e_{2i}\tanh(\frac{e_{2i}}{b})] \tag{26}$$

$$0 \leq |x| - x\tanh(\frac{x}{b}) \leq 0.2785b, \forall b > 0, x \in R \tag{27}$$

we obtain

$$\begin{aligned}
\dot{V}_3 &\leq -e_1^T K_1 e_1 - e_2^T K_2 e_2 + \lambda_\beta \sum_{i=1}^{n} [|e_{2i}| - e_{2i} \tanh(\frac{e_{2i}}{b})] \\
&\quad -\frac{\sigma_w}{2}\|\tilde{W}\|_F^2 + \frac{\sigma_w}{2}\|W^*\|_F^2 - \frac{\sigma_\beta}{2}\|\tilde{\beta}\|_F^2 + \frac{\sigma_\beta}{2}\|\beta^*\|_F^2 \\
&\leq -e_1^T K_1 e_1 - e_2^T K_2 e_2 - \frac{\sigma_w}{2}\|\tilde{W}\|_F^2 - \frac{\sigma_\beta}{2}\|\tilde{\beta}\|_F^2 \\
&\quad +0.2785nb\lambda_\beta + \frac{\sigma_\beta}{2}\|\beta^*\|_F^2 + \frac{\sigma_w}{2}\|W^*\|_F^2 \\
&\leq -\rho_1 V_3 + C_1 \qquad (28)
\end{aligned}$$

where

$$\rho_1 = \min\{2\lambda_{\min}(K_1), \frac{2h_a^*\lambda_{\min}(K_2)}{m^*}, \frac{\sigma_w}{\lambda_{\max}(\Gamma_w^{-1})}, \frac{\sigma_\beta}{\lambda_{\max}(\Gamma_\beta^{-1})}\} \qquad (29)$$

$$C_1 = 0.2785nb\lambda_\beta + \frac{\sigma_w}{2}\|W^*\|_F^2 + \frac{\sigma_\beta}{2}\|\beta^*\|_F^2 \qquad (30)$$

K_1 and K_2 are chosen as

$$\lambda_{\min}(K_1) > 0, \quad \lambda_{\min}(K_2) > 0 \qquad (31)$$

Remark 1. Exponential stability could be achieved if $C_1 = 0$. For the proposed controller however, $C_1 = 0.2785nb\lambda_\beta + \frac{\sigma_w}{2}\|W^*\|_F^2 + \frac{\sigma_\beta}{2}\|\beta^*\|_F^2$, where σ_β and σ_w are constant control parameters. These parameters help make the system more robust. If these parameters are set to zero, the term remaining is $0.2785nb\lambda_\beta$, which is greater than zero. The system can therefore not achieve exponential stability.

Theorem 1. When initial conditions of the robotic manipulator system (1), full state feedback control law (19) and adaptation laws (20) and (21) are bounded, there exist constant matrices $K_1 > 0$, $K_2 > 0$, $\Gamma_w > 0$, $\Gamma_\beta > 0$, $\sigma_w > 0$ and $\sigma_\beta > 0$ such that the closed-loop system is semi-globally stable.

Proof: The proof of the above theorem is given in the appendix.

3.2. Output Feedback Control

The system states are considered to be measurable for the state feedback controller. It is however impractical to do so [40–42]. An output feedback controller is designed in this section, where, a high gain observer estimates unmeasurable state terms [43]. x_2 is denoted as $\frac{\pi_2}{\epsilon}$ [44]. e_2 can therefore be estimated as

$$\hat{e}_2 = \frac{\pi_2}{\epsilon} - \alpha \tag{32}$$

where the dynamics of π_2 is described as

$$\epsilon\dot{\pi}_1 = \pi_2 \tag{33}$$

$$\epsilon\dot{\pi}_2 = \lambda_1\pi_2 - \pi_1 + x_1 \tag{34}$$

where ϵ and λ_1 are positive constants. According to [45], we have

$$\xi_2 = \frac{\pi_2}{\epsilon} - \dot{x}_1 = -\epsilon\psi^{(2)} \tag{35}$$

$$\tilde{e}_2 = \hat{e}_2 - e_2 = \frac{\pi_2}{\epsilon} - \alpha - \dot{x}_1 + \alpha = \xi_2 \tag{36}$$

Therefore, we can use $\frac{\pi_2}{\epsilon}$ to estimate $\dot{x}_1$ and x_2, e_2 can be estimated as follows

$$\hat{x}_2 = \frac{\pi_2}{\epsilon} \tag{37}$$

$$\hat{e}_2 = \frac{\pi_2}{\epsilon} - \alpha \tag{38}$$

Using control law (19) and the neural network updating laws (20) and (21), we write the output feedback controller and its update laws are written as:

$$\begin{aligned} \tau &= -e_1 - K_2\hat{e}_2 - \hat{W}^T S(\hat{X}) - \hat{\beta}\tanh(\frac{\hat{e}_2}{b}) && (39)\\ \dot{\hat{W}} &= \Gamma_w(S(\hat{X})\hat{e}_2^T - \sigma_w\hat{W}) && (40)\\ \dot{\hat{\beta}} &= \Gamma_\beta(\tanh(\frac{\hat{e}_2}{b})\hat{e}_2^T - \sigma_\beta\hat{\beta}) && (41) \end{aligned}$$

Consider the Lyapunov function

$$V_3 = V_2 + tr\{\frac{1}{2}\tilde{W}^T\Gamma_w^{-1}\tilde{W}\} + tr\{\frac{1}{2}\tilde{\beta}^T\Gamma_\beta^{-1}\tilde{\beta}\} \quad (42)$$

Differentiating (42) yields

$$\dot{V}_3 = \dot{V}_2 + tr\{\tilde{W}^T\Gamma_w^{-1}\dot{\hat{W}}\} + tr\{\tilde{\beta}^T\Gamma_\beta^{-1}\dot{\hat{\beta}}\} \quad (43)$$

Substituting (18) into (43) yields

$$\dot{V}_3 = -e_1^T K_1 e_1 + e_1^T e_2 + e_2^T[\tau + Q(X) + H_a^{-1}D(\tau)] + tr\{\tilde{W}^T\Gamma_w^{-1}\dot{\hat{W}}\} + tr\{\tilde{\beta}^T\Gamma_\beta^{-1}\dot{\hat{\beta}}\}$$

where $Q(X)$ is expressed as

$$Q(X) = W^{*T}S(\hat{X}) + \epsilon_z \quad (44)$$

Substituting (44) and (39) into (43) yields

$$\begin{aligned} \dot{V}_3 = &-e_1^T K_1 e_1 + e_2^T[-K_2\hat{e}_2 - \hat{\beta}\tanh(\frac{\hat{e}_2}{b}) - \tilde{W}^T S(\hat{X})\\ &+\epsilon_z + H_a^{-1}D(\tau)] + tr\{\tilde{W}^T\Gamma_w^{-1}\dot{\hat{W}}\} + tr\{\tilde{\beta}^T\Gamma_\beta^{-1}\dot{\hat{\beta}}\} \quad (45) \end{aligned}$$

Substituting (40) and (41) into (45) yields

$$\begin{aligned}\dot{V}_3 &= -e_1^T K_1 e_1 - e_2^T K_2 \hat{e}_2 + e_2^T[-\hat{\beta}\tanh(\frac{\hat{e}_2}{b}) - \tilde{W}^T S(\hat{X}) \\ &\quad +\epsilon_z + H_a^{-1} D(\tau)] + tr\{\tilde{W}^T(S(\hat{X})\hat{e}_2^T - \sigma_w \hat{W})\} \\ &\quad +tr\{\tilde{\beta}^T(\tanh(\frac{\hat{e}_2}{b})\hat{e}_2^T - \sigma_\beta \hat{\beta})\} \end{aligned} \tag{46}$$

Denoting $\hat{e}_2 = \tilde{e}_2 + e_2$ and substituting it into equation (46) yields

$$\begin{aligned}\dot{V}_3 &= -e_1^T K_1 e_1 - e_2^T K_2 \tilde{e}_2 - e_2^T K_2 e_2 - \hat{e}_2^T \beta^* \tanh(\frac{\hat{e}_2}{b}) + \tilde{e}_2^T(\hat{\beta})\tanh(\frac{\hat{e}_2}{b}) \\ &\quad +\tilde{e}_2^T \tilde{W}^T S(\hat{X}) + e_2^T[\epsilon_z + H_a^{-1} D(\tau)] - \sigma_w tr\{\tilde{W}^T \hat{W}\} - \sigma_\beta tr\{\tilde{\beta}^T \hat{\beta}\}\end{aligned}$$

$\beta = \epsilon_z + H_a^{-1} D(\tau) \triangleq [\beta_1, \beta_2, ...\beta_n]^T$. The following property holds: $|\beta_i| \leq \|\beta\| \leq \|\epsilon_z\| + \|H_a^{-1}\|\|D(\tau)\| \leq \lambda_\beta, \forall_i = 1, 2, ...n$. This implies that

$$e_2^T[\epsilon_z + H_a^{-1} D(\tau)] = \sum_{i=1}^{n} e_{2i}\beta_i \leq \lambda_\beta \sum_{i=1}^{n} |e_{2i}| \tag{47}$$

Considering (47) and applying the following inequalities we have

$$-\sigma_w tr\{\tilde{W}^T \hat{W}\} \leq -\frac{\sigma_w}{2}\|\tilde{W}\|_F^2 + \frac{\sigma_w}{2}\|W^*\|_F^2 \tag{48}$$

$$-\sigma_\beta tr\{\tilde{\beta}^T \hat{\beta}\} \leq -\frac{\sigma_\beta}{2}\|\tilde{\beta}\|_F^2 + \frac{\sigma_\beta}{2}\|\beta^*\|_F^2 \tag{49}$$

$$-e_2^T K_2 \tilde{e}_2 \leq \frac{1}{2} e_2^T e_2 + \frac{1}{2}(K_2\tilde{e}_2)^T(K_2\tilde{e}_2) \tag{50}$$

we have

$$\begin{aligned}\dot{V}_3 &\leq -e_1^T K_1 e_1 + \frac{1}{2}(K_2\tilde{e}_2)^T(K_2\tilde{e}_2) - e_2^T(K_2 - \frac{1}{2}I)e_2 + \lambda_\beta \sum_{i=1}^{n}(|\hat{e}_{2i}| - \hat{e}_{2i}\tanh(\frac{\hat{e}_{2i}}{b})) \\ &\quad +\lambda_\beta \sum_{i=1}^{n} |\tilde{e}_{2i}|(1 + \tanh(\frac{\hat{e}_{2i}}{b})) + \frac{\sigma_\beta}{2}\|\beta^*\|_F^2 + \|\tilde{\beta}\| \sum_{i=1}^{n} |\tilde{e}_{2i}|\tanh(\frac{\hat{e}_{2i}}{b}) \\ &\quad +\sum_{i=1}^{n} \tilde{W}_i^T S_i(\hat{X})\tilde{e}_{2i} - \frac{\sigma_w}{2}\|\tilde{W}\|_F^2 + \frac{\sigma_w}{2}\|W^*\|_F^2 - \frac{\sigma_\beta}{2}\|\tilde{\beta}\|_F^2 \end{aligned} \tag{51}$$

However

$$
\begin{aligned}
0 &\leq |x| - x\tanh(\frac{x}{b}) \leq 0.2785b && (52)\\
0 &\leq 1 + \tanh(x) \leq 2 && (53)\\
-1 &\leq \tanh(x) \leq 1 && (54)\\
\tilde{W}_i^T S_i(\hat{X})\tilde{e}_{2i} &\leq \frac{\sigma_{wi}}{4} \parallel \tilde{W}_i \parallel^2 + \frac{1}{\sigma_{wi}} \parallel S_i(\hat{X}) \parallel^2 \tilde{e}_{2i}^2
\end{aligned}
$$

Substituting $\parallel S_i(\hat{X}) \parallel^2 \leq l_i$ into (55) yields

$$
\tilde{W}_i^T S_i(\hat{X})\tilde{e}_{2i} \leq \frac{\sigma_{wi}}{2} \parallel \tilde{W}_i \parallel^2 + \frac{2l_i}{\sigma_{wi}}\frac{1}{4}\tilde{e}_{2i}^2 \quad (55)
$$

Substituting (52), (53), (54) and (55) into (51) yields

$$
\begin{aligned}
\dot{V}_3 \leq\ & -e_1^T K_1 e_1 - e_2^T(K_2 - \frac{1}{2}I)e_2 + 0.2785bn\lambda_\beta \\
& + \frac{1}{2}\tilde{e}_2^T(K_2^T K_2 + \mathrm{diag}(2l_i/\sigma_{wi}))\tilde{e}_2 + \|\tilde{\beta}\| \sum_{i=1}^{n} |\tilde{e}_{2i}| + 2\lambda_\beta \sum_{i=1}^{n} |\tilde{e}_{2i}| \\
& + \sum_{i=1}^{n} \frac{\sigma_{wi}}{4}\|\tilde{W}_i\|^2 - \frac{\sigma_w}{2}\|\tilde{W}\|_F^2 + \frac{\sigma_w}{2}\|W^*\|_F^2 - \frac{\sigma_\beta}{2}\|\tilde{\beta}\|_F^2 + \frac{\sigma_\beta}{2}\|\beta^*\|_F^2 \qquad (56)
\end{aligned}
$$

Substituting (36) into (56) and applying $\frac{1}{2}\xi_2^T\xi_2 \leq \frac{1}{2}\epsilon^2 h_2^T h_2$, where $h_2 = [h_{21}, h_{22}, ...h_{2n}]^T$ yields

$$
\begin{aligned}
\dot{V}_3 \leq\ & -e_1^T K_1 e_1 - e_2^T(K_2 - I)e_2 + 0.2785bn\lambda_\beta \\
& + (K_2^T K_2 + \mathrm{diag}(2l_i/\sigma_{wi}))\frac{1}{2}\epsilon^2 h_2^T h_2 - \sum_{i=1}^{n} \frac{\sigma_{wi}}{4}\|\tilde{W}_i\|^2 \\
& + 2\lambda_\beta \sum_{i=1}^{n} |\epsilon h_{2i}| + \|\tilde{\beta}\| \sum_{i=1}^{n} |\epsilon h_{2i}| + \frac{\sigma_w}{2}\|W^*\|_F^2 - \frac{\sigma_\beta}{2}\|\tilde{\beta}\|_F^2 + \frac{\sigma_\beta}{2}\|\beta^*\|_F^2
\end{aligned}
$$

Lemma 1. [46] For the adaptive law (40), there exists a compact set

$$
\Omega_\beta = \{\hat{\beta} | \|\hat{\beta}\| \leq \frac{\vartheta}{\kappa}\} \quad (57)
$$

where $\| \tanh(\frac{\hat{e}_2}{b})\| \leq \vartheta$ with $\kappa > 0$, such that $\hat{\beta}(t) \in \Omega_\beta$, $\forall t \geq 0$ provided $\hat{\beta}(0) \in \Omega_\beta$

From Lemma 1,

$$\|\tilde{\beta}\| = \|\hat{\beta} - \beta^*\| \leq \|\hat{\beta}\| + \|\beta^*\| \leq \frac{\vartheta}{\kappa} + \|\beta^*\| \tag{58}$$

Thus we can obtain

$$\dot{V}_3 \leq -\rho_2 V_3 + C_2 \tag{59}$$

where

$$\begin{aligned}
\rho_2 &= \min\{2\lambda_{\min}(K_1), \frac{2h_a^*\lambda_{\min}(K_2 - I)}{m^*}, \frac{\sigma_w}{\lambda_{\max}(\Gamma_w^{-1})}, \frac{\sigma_\beta}{\lambda_{\max}(\Gamma_\beta^{-1})}\} \\
C_2 &= 0.2785nb\lambda_\beta + \frac{\sigma_\beta}{2}\|\beta^*\|_F^2 + \frac{\sigma_w}{2}\|W^*\|_F^2 + (\frac{\vartheta}{\kappa} + \|\beta^*\|)\sum_{i=1}^{n}|\epsilon h_{2i}| \\
&\quad +2\lambda_\beta \sum_{i=1}^{n}|\epsilon h_{2i}| + (K_2^T K_2 + \mathrm{diag}(2l_i/\sigma_{wi}))\frac{1}{2}\epsilon^2 h_2^T h_2
\end{aligned} \tag{60}$$

where K_1 and K_2 are chosen as

$$\lambda_{\min}(K_1) > 0, \quad \lambda_{\min}(K_2 - I) > 0 \tag{61}$$

Remark 2. Exponential stability could be achieved if $C_2 = 0$. For the proposed controller however, $C_2 = 0.2785nb\lambda_\beta + \frac{\sigma_\beta}{2}\|\beta^*\|_F^2 + \frac{\sigma_w}{2}\|W^*\|_F^2 + 2\lambda_\beta \sum_{i=1}^{n}|\epsilon h_{2i}| + \|\tilde{\beta}\| \sum_{i=1}^{n}|\epsilon h_{2i}| + (K_2^T K_2 + \mathrm{diag}(2l_i/\sigma_{wi}))\frac{1}{2}\epsilon^2 h_2^T h_2$, where σ_β and σ_w are constant control parameters. If these parameters are set to zero, there are terms remaining such as $0.2785nb\lambda_\beta$ and $2\lambda_\beta \sum_{i=1}^{n}|\epsilon h_i|$, which are greater than zero. The system can therefore not achieve exponential stability.

Theorem 2. When initial conditions of the robotic manipulator system (1), output feedback control (39) and adaptation laws (40) and (41) are bounded, there exist constant matrices $K_1 > 0$, $(K_2 - I) > 0$, $\Gamma_w > 0$, $\Gamma_\beta > 0$, $\sigma_w > 0$ and $\sigma_\beta > 0$ such the closed loop system is semi-globally stable.

The proof of Theorem 2 has been omitted since it is quite similar to that of theorem 1. Fig. 2

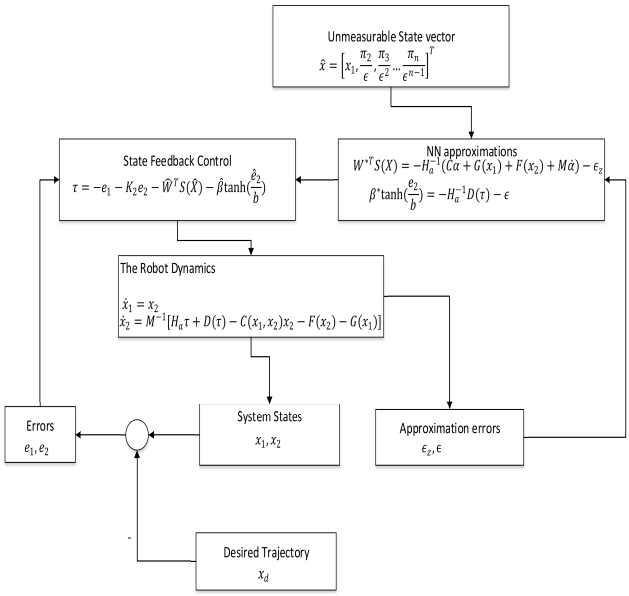

Fig. 2. *Output feedback control strategy*

shows the strategy for the output feedback control.

4. Simulation

Using simulations, the effectiveness of our proposed controllers is illustrated. The robot has two rotary joints and one prismatic joint. $M(x_1)$, $C(x_1, x_2)$ and $G(x_1)$ are expressed as

$$M(x_1) = \begin{bmatrix} M_{11} & M_{12} & M_{13} \\ M_{21} & M_{22} & 0 \\ M_{31} & 0 & M_{33} \end{bmatrix} \tag{62}$$

$$C(x_1, x_2) = \begin{bmatrix} C_{11} & C_{12} & C_{13} \\ C_{21} & C_{22} & C_{23} \\ C_{31} & C_{32} & 0 \end{bmatrix} \tag{63}$$

$$G(x_1) = \begin{bmatrix} 0 \\ G_{21} \\ G_{31} \end{bmatrix} \tag{64}$$

Where $M_{11} = m_3 q_3^2 \sin q_2^2 + m_3 l_1^2 + m_2 l_1^2 + I_1$, $M_{12} = M_{21} = m_3 q_3 l_1 \cos q_2$, $M_{13} = M_{31} = m_3 l_1 \sin q_2$, $M_{22} = m_3 q_3^2 + I_2$, $M_{33} = m_3$, $C_{11} = m_3 q_3^2 \sin q_2 \cos q_2 \dot{q}_2 + m_3 q_3 \sin q_2^2 \dot{q}_3$, $C_{12} = m_3 q_3^2 \sin q_2 \cos q_2 \dot{q}_1 - m_3 l_1 q_3 \sin q_2 \dot{q}_2 - m_3 l_1 q_3 \sin q_2 \dot{q}_3$, $C_{13} = m_3 q_3 \sin q_2^2 \dot{q}_1 - m_3 l_1 q_3 \sin q_2 \dot{q}_2$, $C_{21} = -m_3 q_3^2 \sin q_2 \cos q_2 \dot{q}_1$, $C_{22} = m_3 q_3 \dot{q}_3$, $C_{23} = m_3 q_3 \dot{q}_2 + m_3 l_1 \cos q_2 \dot{q}_3$, $C_{31} = -m_3 q_3 \sin q_2^2 \dot{q}_1 + m_3 l_1 \cos q_2 \dot{q}_2$, $C_{32} = m_3 l_1 \cos q_2 \dot{q}_1 - m_3 q_3 \dot{q}_2$, $G_{21} = -m_3 g q_3 \cos q_2$, $G_{31} = -m_3 g \sin q_2$. $m_1 = 1$kg, $m_2 = 0.85$kg, $m_3 = 1$kg, $l_1 = 0.3$m, $l_2 = 0.4$m, $l_3 = 0.5$m. The friction term is defined as $F(\dot{q}) = F_v \dot{q} + F_d(\dot{q}) = \mathrm{diag}[2, 2]\dot{q} + 1.5\mathrm{sgn}(\dot{q})$, and sgn($x$) is defined as

$$\mathrm{sgn}(k) = \begin{cases} -1, & \text{if } k \geq 0 \\ +1, & \text{otherwise} \end{cases} \tag{65}$$

All initial positions of the robot is set at 0. The desired trajectory is chosen as

$$q_d = [0.1\cos(0.5t), 0.1\sin(0.5t), 0.1 + 0.1\cos(0.5t)] \tag{66}$$

The control gains are chosen as $K_1 = \text{diag}[5, 5, 5]$ and $K_2 = \text{diag}[20, 20, 20]$. Sixteen nodes are used, variance $= 50$, $\sigma_\beta = \sigma_w = 0.01$, $\Gamma_\beta = 50I_{3\times3}$, $\Gamma_w = 50I_{16\times16}$. The neural network weights are initialized from zero, $\epsilon = 0.005$, $\lambda = [5, 5, 5]$. The high gain observer is also initialized from zero. The diagram of the 3-DOF robotic manipulator is shown in Fig. 4. In this paper sixteen

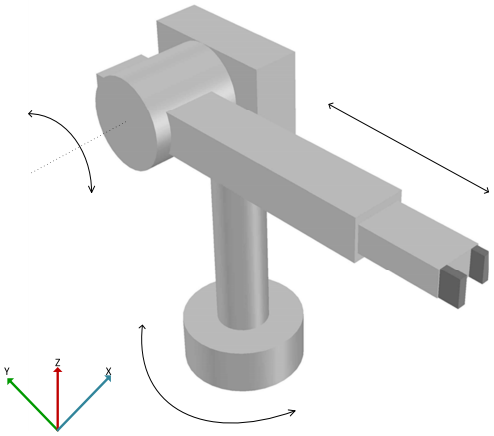

Fig. 3. *Diagram of a 3-DOF robotic manipulator*

hidden-layer neurons are used for the RBF neural network and three hidden-layer neurons are used for the tanh network.

Determining the number of hidden layer neurons required for any application is an open problem. One can perform computer simulations of the controller and then increase the number for another simulation run. If no further improvement is detected, that value of hidden nodes can be used. Increasing the number of neural network nodes will however increase the computation time of your code. The type of activation function used and the number of input selected can also determine the number of neural network nodes. The design parameters such as K_1, K_2, σ_w, σ_β, has great effect on the tracking performance. Increasing or decreasing them can result in either small or large tracking errors. The values used in this work were chosen through trial and error method. However, we are working on formulating it as an optimization problem, which chooses optimum parameters for excellent tracking performance. The radial basis function neural network is a higher order network that approximates the dynamics of the robot. The term $\hat{\beta}\tanh(\frac{e_2}{b})$ is a high gain term that counteracts the term associated with the upper bound on the term $\|H_a^{-1}\|D^*$.

We compared our state and output feedback controllers with controllers without backlash hys-

teresis compensation. The tracking performance of the controllers with backlash-hysteresis compensation is shown in Fig. 4. The neural network successfully approximates the dynamics of the robot and the hysteresis nonlinearity. From Fig. 4 the controllers show excellent tracking performance. In Fig. 5, it can be seen that the absolute values of the tracking errors also converge to a very small value or is less than a small value closer to zero. The closed loop system therefore remains bounded for all time. The tracking performance of the controllers without backlash compensation in Fig. 9 shows a more oscillatory and bad tracking performance. The controller tries to track the desired trajectory but is unable to do so. This is due to the absence of the high gain term $\hat{\beta}\tanh(\frac{\hat{e}_2}{b})$.

The errors of the controllers without backlash compensation, in Fig. 10 are more oscillatory and larger in magnitude than the errors of the controllers with backlash compensation. This shows that the RBF neural network alone, is not able to approximate the backlash hysteresis nonlinearity. The addition of the $\tanh$ neural network however ensures the compensation of hysteresis and good tracking performance. Backlash hysteresis therefore needs to be compensated in robotic manipulators. The values of the control input for controllers without backlash compensation are also higher than the compensated controllers. The norms of the neural network weights of the compensated controllers are smoother than the weights of the uncompensated controllers. The torque inputs in Fig. 6 and Fig. 11 are also within realistic ranges, hence the controller can be implemented.

5. Conclusion

An adaptive neural network controller has been designed for a 3-DOF robotic manipulator. The controller mitigates the effects of backlash-like hysteresis. State and output feedback control schemes have been considered. The dynamics of the robot has been approximated by a neural network which uses a radial basis function. The unknown hysteresis nonlinearity is approximated by another neural network that employs a hyperbolic tangent activation function. A high gain observer is used in the output feedback controller design to estimate system states. The proposed control schemes are all verified through simulations and compared with controllers without hysteresis

compensation. Future work will include the investigation of other intelligent control schemes, their implementation on real robotic systems, optimizing neural network controller parameters.

Acknowledgement

The authors thank the editor-In-chief, associate editor and the reviewers for their constructive comments which helped improve the quality of this paper.

Appendix

Theorem 1 Proof

Proof 1. Multiplying (28) by $e^{\rho_1 t}$ yields

$$\frac{d}{dt}(V_3 e^{\rho_1 t}) \leq C_1 e^{\rho_1 t} \tag{67}$$

Integrating yields

$$0 \leq V_3(t) \leq \frac{C_1}{\rho_1} + [V_3(0) - \frac{C_1}{\rho_1}]e^{-\rho_1 t} \tag{68}$$

This implies that e_1, e_2 and $\tilde{W}$ are uniformly ultimately bounded. Given the constants, b, σ_w and σ_β, the value of $\frac{C_1}{\rho_1}$ can be made arbitrarily small by increasing $\lambda_{\min}(K_1)$ and $\lambda_{\min}(K_2)$ and the tracking error e_1 can be made small.

6. References

[1] G. Tao and P. Kokotovic, "Adaptive control of plants with unknown hystereses," *IEEE Transactions on Automatic Control*, vol. 40, no. 2, pp. 200–212, Feb 1995.

[2] Q. Wang, C.-Y. Su, and Y. Tan, "On the control of plants with hysteresis: overview and a prandtl-ishlinskii hysteresis based control approach," *Acta automatica sinica*, vol. 31, no. 1,

pp. 92–104, Jan 2005.

[3] C.-Y. Su, M. Oya, and H. Hong, "Stable adaptive fuzzy control of nonlinear systems preceded by unknown backlash-like hysteresis," *IEEE Transactions on Fuzzy Systems*, vol. 11, no. 1, pp. 1–8, Feb 2003.

[4] Y. Liu and Y. Lin, "Global adaptive output feedback tracking for a class of non-linear systems with unknown backlash-like hysteresis," *IET Control Theory Applications*, vol. 8, no. 11, pp. 927–936, July 2014.

[5] M. Ruderman, F. Hoffmann, and T. Bertram, "Modeling and identification of elastic robot joints with hysteresis and backlash," *IEEE Transactions on Industrial Electronics*, vol. 56, no. 10, pp. 3840–3847, Oct 2009.

[6] G.-Y. Gu, L.-M. Zhu, and C.-Y. Su, "Modeling and compensation of asymmetric hysteresis nonlinearity for piezoceramic actuators with a modified prandtl–ishlinskii model," *IEEE Transactions on Industrial Electronics*, vol. 61, no. 3, pp. 1583–1595, March 2014.

[7] S. Rosenbaum, M. Ruderman, T. Strohla, and T. Bertram, "Use of jiles–atherton and preisach hysteresis models for inverse feed-forward control," *IEEE Transactions on Magnetics*, vol. 46, no. 12, pp. 3984–3989, Dec 2010.

[8] G. Song, J. Zhao, X. Zhou, D. Abreu-Garcia, *et al.*, "Tracking control of a piezoceramic actuator with hysteresis compensation using inverse preisach model," *IEEE/ASME Transactions on Mechatronics*, vol. 10, no. 2, pp. 198–209, April 2005.

[9] J. Yi, S. Chang, and Y. Shen, "Disturbance-observer-based hysteresis compensation for piezoelectric actuators," *IEEE/ASME Transactions on Mechatronics*, vol. 14, no. 4, pp. 456–464, Aug 2009.

[10] K. M. Tsang and G. Li, "Robust nonlinear nominal-model following control to overcome deadzone nonlinearities," *IEEE Transactions on Industrial Electronics*, vol. 48, no. 1, pp. 177–184, Feb 2001.

[11] T.-C. Lee, K.-T. Song, C.-H. Lee, and C.-C. Teng, "Tracking control of unicycle-modeled mobile robots using a saturation feedback controller," *IEEE Transactions on Control Systems Technology*, vol. 9, no. 2, pp. 305–318, Mar 2001.

[12] L. Cheng, W. Liu, Z. G. Hou, J. Yu, and M. Tan, "Neural-network-based nonlinear model predictive control for piezoelectric actuators," *IEEE Transactions on Industrial Electronics*, vol. 62, no. 12, pp. 7717–7727, Dec 2015.

[13] C.-Y. Su, Y. Stepanenko, J. Svoboda, and T.-P. Leung, "Robust adaptive control of a class of nonlinear systems with unknown backlash-like hysteresis," *IEEE Transactions on Automatic Control*, vol. 45, no. 12, pp. 2427–2432, Dec 2000.

[14] J. Zhou, C. Wen, and Y. Zhang, "Adaptive backstepping control of a class of uncertain nonlinear systems with unknown backlash-like hysteresis," *IEEE Transactions on Automatic Control*, vol. 49, no. 10, pp. 1751–1759, Oct 2004.

[15] Y. Li and S. Tong, "Adaptive fuzzy output constrained control design for multi-input multi-output stochastic nonstrict-feedback nonlinear systems," *IEEE Transactions on Cybernetics*, vol. PP, no. 99, pp. 1–10, 2016.

[16] Y. Li, S. Tong, and T. Li, "Observer-based adaptive fuzzy tracking control of mimo stochastic nonlinear systems with unknown control directions and unknown dead zones," *IEEE Transactions on Fuzzy Systems*, vol. 23, no. 4, pp. 1228–1241, Aug 2015.

[17] J. Zhou, C. Zhang, and C. Wen, "Robust adaptive output control of uncertain nonlinear plants with unknown backlash nonlinearity," *IEEE Transactions on Automatic Control*, vol. 52, no. 3, pp. 503–509, March 2007.

[18] W. He, A. O. David, Z. Yin, and C. Sun, "Neural network control of a robotic manipulator with input deadzone and output constraint," *Systems, IEEE Transactions on Systems, Man, and Cybernetics*, vol. 46, no. 6, pp. 759–770, June 2016.

[19] Y. Li, S. Sui, and S. Tong, "Adaptive fuzzy control design for stochastic nonlinear switched systems with arbitrary switchings and unmodeled dynamics," *IEEE Transactions on Cybernetics*, vol. PP, no. 99, pp. 1–12, 2016.

[20] A. Sen and R. Johnson, "A nonlinear compensation technique for systems involving hysteresis," *IEEE Transactions on Automatic Control*, vol. 13, no. 6, pp. 711–714, Dec 1968.

[21] Y. J. Liu, L. Tang, S. Tong, C. L. P. Chen, and D. J. Li, "Reinforcement learning design-based adaptive tracking control with less learning parameters for nonlinear discrete-time mimo systems," *IEEE Transactions on Neural Networks and Learning Systems*, vol. 26, no. 1, pp. 165–176, Jan 2015.

[22] R. Lu, Z. Li, C.-Y. Su, and A. Xue, "Development and learning control of a human limb with a rehabilitation exoskeleton," *IEEE Transactions on Industrial Electronics*, vol. 61, no. 7, pp. 3776–3785, July 2014.

[23] X. Bu, Z. Hou, F. Yu, and Z. Fu, "Brief paper: iterative learning control for a class of nonlinear switched systems," *IET Control Theory Applications*, vol. 7, no. 3, pp. 470–481, February 2013.

[24] C. Yang, X. Wang, L. Cheng, and H. Ma, "Neural-learning based telerobot control with guaranteed performance," *IEEE Transactions on Cybernetics*, DOI: 10.1109/TCYB.2016.2573837, 2014.

[25] C. Yang, Z. Li, R. Cui, and B. Xu, "Neural network-based motion control of an underactuated wheeled inverted pendulum model," *IEEE Transactions on Neural Networks and Learning Systems*, vol. 25, no. 11, pp. 2004–2016, 2014.

[26] Z. Li and C.-Y. Su, "Neural-adaptive control of single-master-multiple-slaves teleoperation for coordinated multiple mobile manipulators with time-varying communication delays and input uncertainties," *IEEE Transactions on Neural Networks and Learning System*, vol. 24, no. 9, pp. 1400–1413, 2013.

[27] L. Cheng, Z.-G. Hou, M. Tan, and W.-J. Zhang, "Tracking control of a closed-chain five-bar robot with two degrees of freedom by integration of an approximation-based approach and mechanical design," *Part B: IEEE Transactions on Systems, Man, and Cybernetics*, vol. 42, no. 5, pp. 1470–1479, Oct 2012.

[28] Z. Liu, C. Chen, Y. Zhang, and C. Chen, "Adaptive neural control for dual-arm coordination of humanoid robot with unknown nonlinearities in output mechanism," *IEEE Transactions on Cybernetics*, vol. 45, no. 3, pp. 521–532, Feb 2015.

[29] R. R. Selmic and F. L. Lewis, "Backlash compensation in nonlinear systems using dynamic inversion by neural networks," *Asian Journal of Control*, vol. 2, no. 2, pp. 76–87, 2000.

[30] G. Jie, L. Xiangdong, L. Xiaozhong, and L. Zhilin, "Neural networks preisach model and inverse compensation for hysteresis of piezoceramic actuator," in *2010 8th World Congress on Intelligent Control and Automation (WCICA)*, July 2010, pp. 5746–5752.

[31] D. R. Seidl, S.-L. Lam, J. Putman, R. D. Lorenz, *et al.*, "Neural network compensation of gear backlash hysteresis in position-controlled mechanisms," *IEEE Transactions on Industry Applications*, vol. 31, no. 6, pp. 1475–1483, Nov 1995.

[32] P. Li, P. Li, and Y. Sui, "Adaptive fuzzy hysteresis internal model tracking control of piezoelectric actuators with nanoscale application," *IEEE Transactions on Fuzzy Systems*, vol. 24, no. 5, pp. 1246–1254, Oct 2016.

[33] Z. Liu, G. Lai, Y. Zhang, X. Chen, and C. L. P. Chen, "Adaptive neural control for a class of nonlinear time-varying delay systems with unknown hysteresis," *IEEE Transactions on Neural Networks and Learning Systems*, vol. 25, no. 12, pp. 2129–2140, Dec 2014.

[34] F. L. Lewis, K. Liu, and A. Yesildirek, "Neural net robot controller with guaranteed tracking performance," *IEEE Transactions on Neural Networks*, vol. 6, no. 3, pp. 703–715, May 1995.

[35] X. Li and C. C. Cheah, "Adaptive neural network control of robot based on a unified objective bound," *IEEE Transactions on Control Systems Technology*, vol. 22, no. 3, pp. 1032–1043, May 2014.

[36] Y. H. Kim and F. L. Lewis, "Neural network output feedback control of robot manipulators," *IEEE Transactions on Robotics and Automation*, vol. 15, no. 2, pp. 301–309, Apr 1999.

[37] W. He, S. S. Ge, B. V. E. How, and Y. S. Choo, *Dynamics and control of mechanical systems in offshore engineering*. Springer, 2014.

[38] W.-D. Zhou, C.-Y. Liao, L. Zheng, and M.-M. Liu, "Adaptive fuzzy output feedback control for a class of nonaffine nonlinear systems with unknown dead-zone input," *Springer, Nonlinear Dynamics*, vol. 79, no. 4, pp. 2609–2621, Dec 2015. [Online]. Available: http://dx.doi.org/10.1007/s11071-014-1835-x

[39] W. He and S. S. Ge, "Vibration control of a flexible beam with output constraint," *IEEE Transactions on Industrial Electronics*, vol. 62, no. 8, pp. 5023–5030, Aug 2015.

[40] Y. J. Liu, S. Tong, D. J. Li, and Y. Gao, "Fuzzy adaptive control with state observer for a class of nonlinear discrete-time systems with input constraint," *IEEE Transactions on Fuzzy Systems*, vol. PP, no. 99, pp. 1–1, 2015.

[41] C. L. P. Chen, G. X. Wen, Y. J. Liu, and Z. Liu, "Observer-based adaptive backstepping consensus tracking control for high-order nonlinear semi-strict-feedback multiagent systems," *IEEE Transactions on Cybernetics*, vol. 46, no. 7, pp. 1591–1601, July 2016.

[42] Y.-J. Liu and S.-C. Tong, "Barrier lyapunov functions-based adaptive control for a class of nonlinear pure-feedback systems with full state constraints," *Automatica*, vol. 64, no. 2, pp. 70–75, 2016.

[43] A. A. Prasov and H. K. Khalil, "A nonlinear high-gain observer for systems with measurement noise in a feedback control framework," *IEEE Transactions on Automatic Control*, vol. 58, no. 3, pp. 569–580, March 2013.

[44] K. P. Tee and S. S. Ge, "Control of fully actuated ocean surface vessels using a class of feedforward approximators," *IEEE Transactions on Control Systems Technology*, vol. 14, no. 4, pp. 750–756, July 2006.

[45] S. S. Ge and J. Zhang, "Neural-network control of nonaffine nonlinear system with zero dynamics by state and output feedback," *IEEE Transactions on Neural Networks*, vol. 14, no. 4, pp. 900–918, July 2003.

[46] W. He, Y. Chen, and Z. Yin, "Adaptive neural network control of an uncertain robot with full-state constraints," *IEEE Transactions on Cybernetics*, vol. 46, no. 3, pp. 620–629, March 2016.

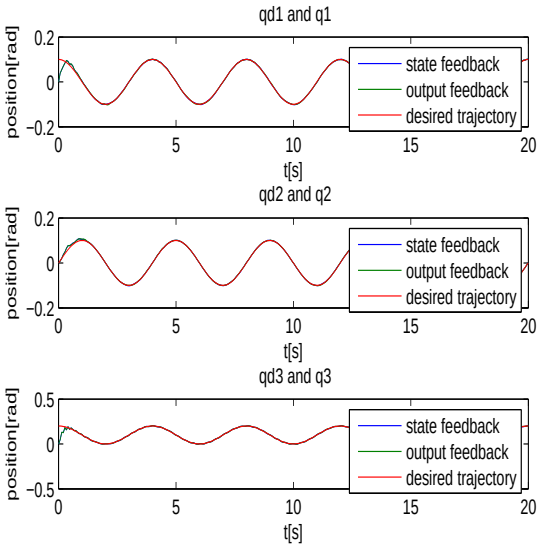

Fig. 4. *Tracking performance (with backlash compensation)*

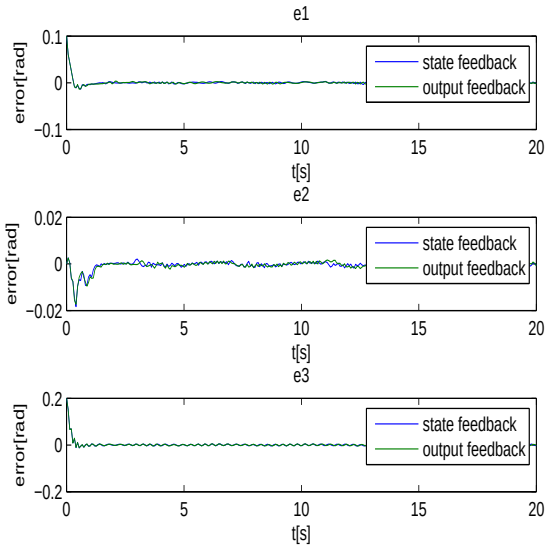

Fig. 5. *Error (with backlash compensation)*

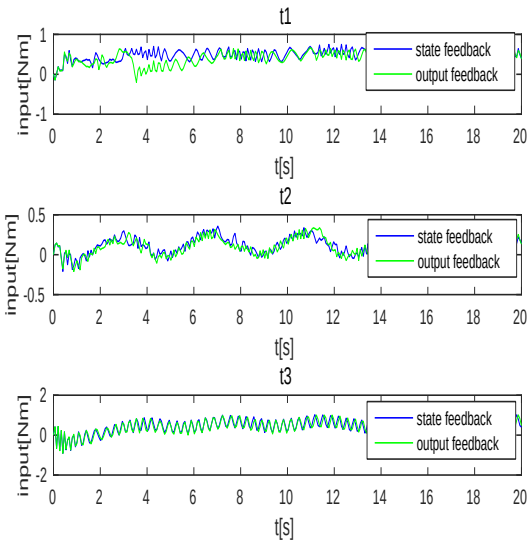

Fig. 6. *Torque (with backlash compensation)*

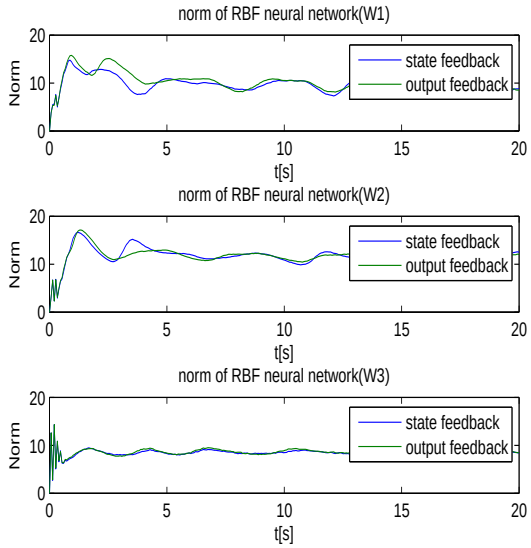

Fig. 7. *Norms of RBF neural network (with backlash compensation)*

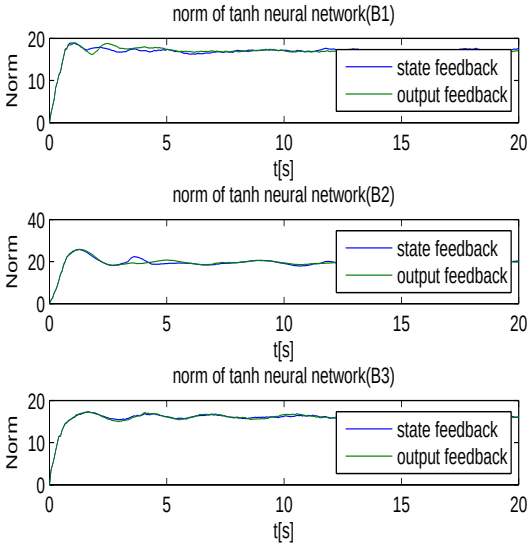

Fig. 8. *Norms of tanh neural network (with backlash compensation)*

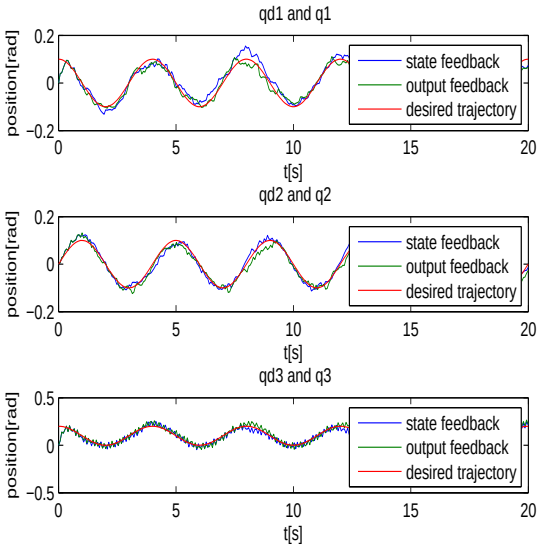

Fig. 9. *Tracking performance (without backlash compensation)*

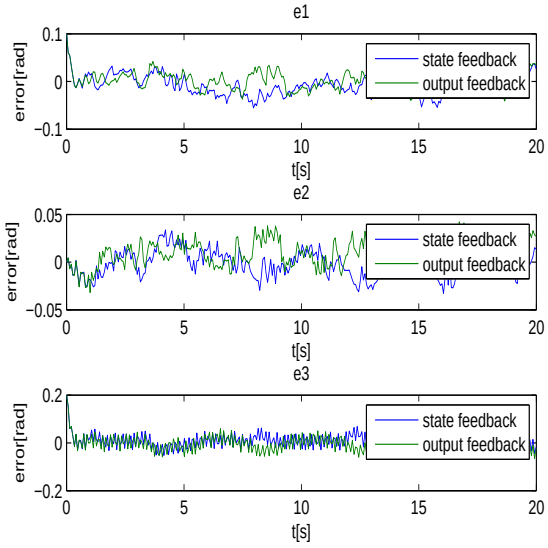

Fig. 10. *Error (without backlash compensation)*

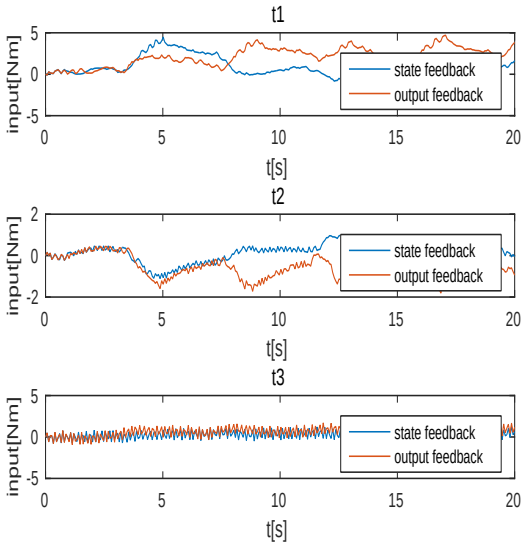

Fig. 11. *Torque (without backlash compensation)*

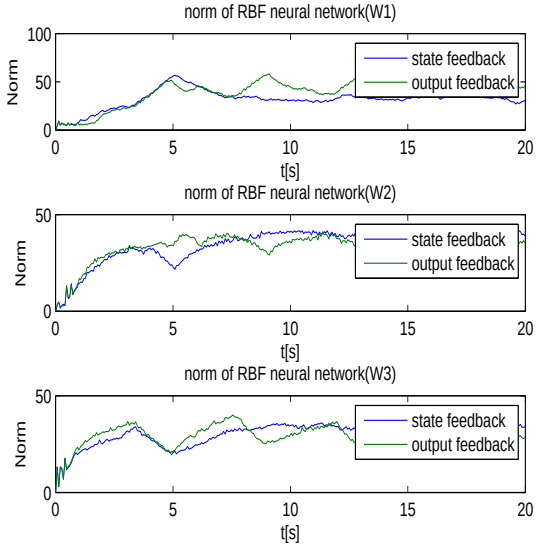

Fig. 12. *Norms of RBF neural network (without backlash compensation)*